

LARGE SCALE EXPERIMENTS OF BURIED STEEL PIPELINES WITH ELBOWS SUBJECTED TO PERMANENT GROUND DEFORMATION

Koji YOSHIKAZAKI¹, Thomas D. O'ROURKE² and Masanori HAMADA³

¹Member of JSCE, M. Eng., Research Engineer, Pipeline Technology Center, Tokyo Gas
(1-7-7, Suehiro-cho, Tsurumi-ku, Yokohama-city, Kanagawa, 230-0045, Japan)

²Member of ASCE, Ph. D., Professor, School of Civil and Environmental Eng., Cornell University
(Hollister Hall, Ithaca, NY 14853, USA)

³Fellow of JSCE, Dr. Eng., Professor, Dept. of Civil Eng., Waseda University
(3-4-1, Okubo, Shinjuku-ku, Tokyo 169-8555, Japan)

Earthquake-induced Permanent Ground Deformation (PGD) can affect significantly underground gas or water pipelines. This paper describes large-scale experiments to investigate the effect of PGD on buried steel pipelines with elbows, and to validate and calibrate Finite Element (FE) modeling. There is good agreement between both the magnitude and distribution of measured strains and deformation and those modeled with FE analyses. The analytical models are able to simulate real performance in a reliable way for dry sand, and for partially saturated sand with an adequate correction factor. Using the analytical model, recommendations are proposed for enhancing the earthquake-resistance of buried pipelines with elbows subjected to PGD.

Key Words: pipeline, elbow, earthquake, gas utility, experiment, FEM, ground deformation, liquefaction, landslide, lifeline, soil-pipe interaction, sand, water content

1. INTRODUCTION

Earthquake-induced Permanent Ground Deformation (PGD), occurring as surface fault deformation, liquefaction-induced soil movements, and landslides, can affect significantly underground lifelines, such as buried gas and water pipelines. There is substantial evidence of gas and water supply pipeline damage caused by PGD from past major earthquakes, such as the 1906 San Francisco^{1,2)}, the 1964 Niigata³⁾, the 1971 San Fernando^{2), 4)}, the 1979 Imperial Valley^{5), 6)}, the 1983 Nihonkai-chubu⁷⁾, the 1989 Loma Prieta⁸⁾, the 1994 Northridge^{6), 9)}, and the 1995 Hyogoken-nanbu¹⁰⁾ earthquakes. More recent earthquakes, including the 1999 Kocaeli and Duzce earthquakes in Turkey, and the 1999 Chi-chi earthquake in Taiwan¹¹⁾, have provided additional evidence of the importance of liquefaction, faults and landslides through their effects on a variety of electrical, gas and water supply lifelines.

Gas and other types of pipelines must often be constructed to change direction rapidly to avoid

other underground facilities or to adjust to the shape of roads under which the pipelines are buried. In such cases the pipeline is installed with an elbow that can be fabricated for a change in direction from 90 to a few degrees. Because elbows are locations where flexural and axial pipeline deformations are restrained, concentrated strains can easily accumulate at elbows in response to PGD.

The response of pipeline elbows, deformed by adjacent ground rupture and subject to the constraining effects of surrounding soil, is a complex interaction problem. A comprehensive and reliable solution to this problem requires laboratory experiments on elbows to characterize their three-dimensional response to axial and flexural loadings, an analytical model that embodies soil-structure interaction combined with three-dimensional elbow response, and full-scale experimental calibration and validation of the analytical model.

Yoshizaki et al.^{12), 13)} have shown a favorable comparison between the results of in-plane bending experiments with elbows and the analytical results

of Finite Element (FE) modeling for strains as high as 30%. A modeling technique, named HYBRID MODEL, was also developed for simulating large-scale pipeline and elbow response to PGD^{14,15}. The model uses shell elements for the elbow where large, localized strains occur. Shell elements are located over a distance of 40 times the pipe diameter from the center point of the elbow. The shell elements are linked to beam elements that extend beyond this distance. Soil-pipeline interaction under PGD is modeled with spring elements in the axial and lateral directions.

Design guidelines¹⁶ refer to the analytical modeling technique for evaluation of pipelines subjected to PGD. Validation of the model is required because high levels of strain can be generated in pipeline elbows by PGD and such levels of strain were not verified experimentally. Suzuki and Ohba¹⁷ investigated cyclic fatigue behavior of a 150-mm-diameter pipeline with an elbow buried with compacted sand subjected to soil displacement of 5 cm, which is specified in design guidelines against earthquakes for gas distribution pipelines¹⁸. The strain generated by this displacement was 2.5 %. Full-scale experimental calibration of the model was therefore undertaken to achieve reliable design procedures for earthquake-resistance against PGD that utilizes the full ductility of the steel.

The objectives of this paper are to describe the results of laboratory full-scale experiments of PGD effects on steel pipelines with elbows, and to refine and validate analytical models so that complex soil-pipeline interactions can be numerically simulated with the precision and reliability necessary for planning and design.

2. LARGE SCALE EXPERIMENTS OF PGD EFFECTS ON PIPELINES

(1) Experimental facility

One of the deformation conditions of interest is illustrated in **Fig. 1** (a) that shows a pipeline with an elbow subjected to PGD consistent with lateral spread and/or landslides. Although lateral spreads and landslides involve complex patterns of soil movement, the most severe deformation associated with these phenomena occurs at the elbows and near the margins between the displaced soil mass and adjacent, more stable ground. The deformation along this boundary can be simplified as abrupt, planar soil displacement. Pipelines that can be designed and sited for abrupt lateral displacement

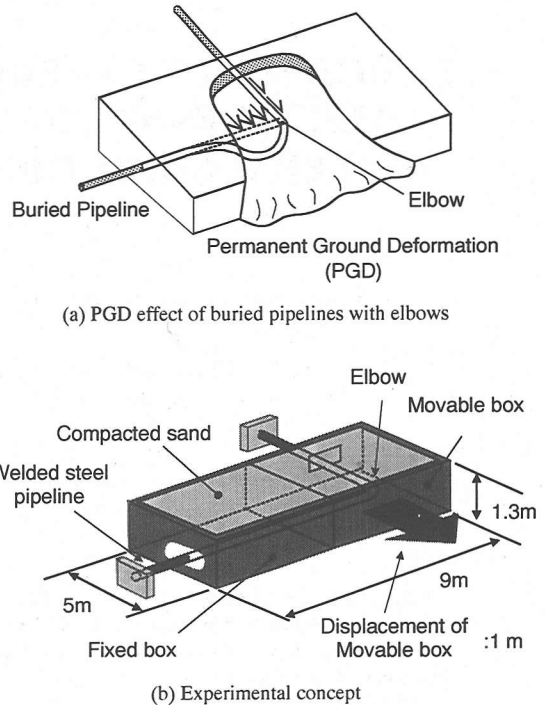


Fig. 1 Experimental concept for PGD effects on buried pipelines with elbows

will be able to accommodate patterns of deformation in the field that frequently involve more gradual distribution of movement across the pipeline. Abrupt soil displacement also represents the principal mode of deformation at fault crossings.

Fig. 1 (b) illustrates the concept of the large-scale experiments. A steel pipeline with an elbow is installed under the actual soil, fabrication, and compaction procedures encountered in practice, and then subjected to lateral soil displacement. The scale of the experimental facility is chosen so that large soil movements are generated, inducing soil-pipeline interaction unaffected by the boundaries of the test facility in which the pipeline is buried. The ground deformation simulated by the experiment represents deformation conditions associated with lateral spread, landslides, and fault crossings. In addition, the experimental data and analytical modeling products are of direct relevance for underground gas, water, petroleum, and electrical conduits.

Fig. 2 shows a plan view of the experimental setup that consisted of five main components, including a test compartment (A and C in the figure), pulley loading system (G), sand storage bin (H), sand container hoisted from storage bin to test

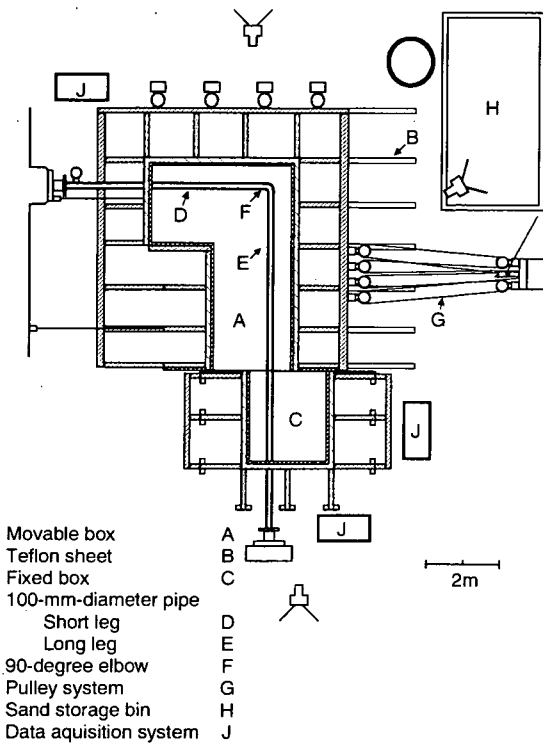


Fig. 2 Plan view of experimental setup

Table 1 Physical properties of Cornell sand

D_{10}	0.2 mm
D_{50}	0.7 mm
D_{60}	0.9 mm
Cu	4.6
Cc	0.9
Classification	SP
Optimum water content	10.1 %
Specific gravity, G_s	2.71
Maximum dry unit weight, $\gamma_{dry, max}$	17.4 kN/m ³

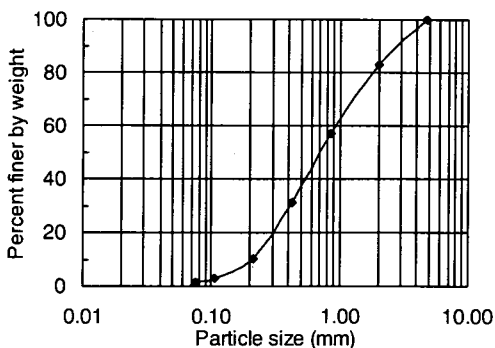


Fig. 3 Grain size distribution of Cornell Sand

compartment (not shown), and data acquisition system (J). The test compartment was composed of a movable box (A) and fixed box (C) within which the instrumented pipeline was installed and backfilled. The L-shaped movable box had inside dimensions of 4.2 m by 6 m by 1.5 m deep. It was constructed on a base of steel I-beams positioned over Teflon sheets that were fixed to the floor. The Teflon sheets provided a low-friction surface on which the moveable box was displaced by a pulley loading system. The fixed box, which was anchored to the floor, was designed to simulate stable ground adjacent to a zone of PGD similar to that illustrated in Fig. 1.

(2) Experimental conditions

A 100-mm-diameter pipeline with 4.1-mm wall thickness was used in the tests. It was composed of two straight pipes welded to a 90-degree elbow (F). The short section of straight pipe (D) was 5.4 m long, whereas the longest section (E) was 9.3 m. Both ends of the pipeline were bolted to reaction walls. The elbows were composed of STPT 370 steel (Japanese Industrial Standard, JIS-G3456) with a specified minimum yield stress of 215 MPa and a minimum ultimate tensile strength of 370 MPa. The straight pipe was composed of SGP steel (JIS-G3452) with a minimum ultimate tensile strength of 294 MPa. About 150 strain gauges were installed on the pipe to measure strain during the tests. Extensometers, load cells, and soil pressure meters were also deployed throughout the test setup.

The pipeline was installed at a 0.9 m depth to top of pipe in each of two experiments. In each experiment soil was placed at a different water content and in situ density. Both experiments were conducted to induce opening-mode deformation of the elbow. They were conducted with an internal nitrogen pressure of 0.1 MPa in the pipeline.

As mentioned above, both ends of the pipeline were bolted to reaction walls so that relatively severe conditions of axial constraint were simulated. Such conditions may occur when a pipeline is effectively anchored by additional elbows, tees, or tie-ins located near the elbow subjected to abrupt soil movement. By calibrating the analytical models for such severe conditions of deformation, the resulting computational tools can be used to simulate wide-ranging field conditions.

Approximately 60 tons of sand were moved from the storage bin into the test compartment for each experiment with a container that was hoisted with the overhead conveyor. The sand is called "Cornell Sand", which is a clean sand (approximately 3% by weight of fines). The properties are summarized in Table 1 and satisfy

Table 2 Experimental condition of sand

	Test 1	Test 2
Water content, w (%)	0.5	3.1
Wet unit weight, γ_{wet} (kN/m ³)	18.4	17.0
Dry unit weight, γ_{dry} (kN/m ³)	18.3	16.7
Friction angle from triaxial compression tests with a strain rate of 0.1%/min (degree)	49	40
Friction angle from triaxial compression tests with a strain rate of 5%/min, (degree)	51	43

0.1%/min	□ $w = 0\%$	× $w = 3\%$	△ $w = 10\%$
5%/min	■ $w = 0\%$	▲ $w = 10\%$	

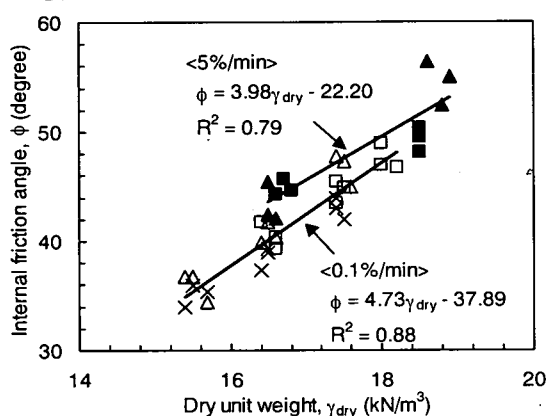


Fig. 4 Relationship between dry unit weight and internal friction angle

the standard for backfill sand specified by Bureau of Construction of Tokyo Metropolitan Government. The grain size curve for the sand is shown in **Fig. 3**. The water content of 0.5% for Test 1 is the hygroscopic water content of the soil, the lowest value possible without oven drying. Hence, the soil in Test 1 is dry sand, and is comparable to the dry sand used in previous soil-pipe interaction tests²⁰. In contrast, Test 2 was performed with sufficiently large water contents to investigate the effects of partial saturation. The tests were performed under carefully controlled conditions of moisture and compaction.

The sand was placed and compacted in 150-mm lifts with strict controls on water content and in situ density, which are summarized in **Table 2**. In this table, internal friction angles obtained from triaxial compression tests with strain rates of 0.1%/min and 5%/min were determined from dry unit weight using the relationship shown in **Fig. 4**. Here, the 0.1%/min is a typical strain rate selected for triaxial compression tests, whereas 5%/min is the maximum

strain rate achieved with the test machine to see the effect of dynamic loading on the results. The relationship between dry unit weight and internal friction angle was the same regardless of water content, as indicated by the triaxial compression test results plotted in **Fig. 4**.

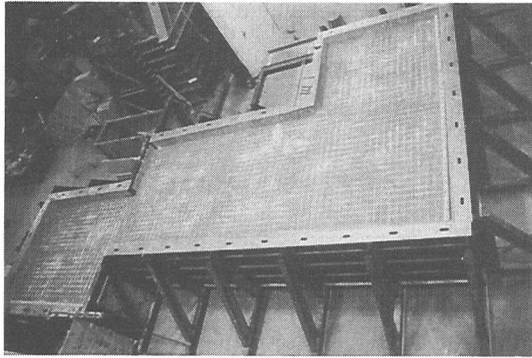
The movable box was pulled by an overhead crane with an 8 to 1 mechanical advantage obtained through the pulley system shown in the figure. The maximum capacity of the loading system was 1 m of lateral displacement and 784 kN. The rate of displacement of the movable box was approximately 16mm/s, which was 1/8 of the speed of the crane wire.

(3) Experimental results

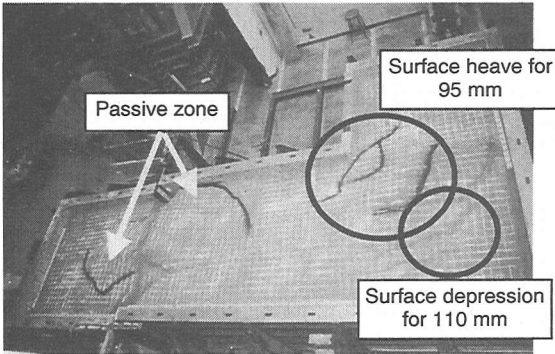
Fig. 5 shows the ground surface of the test compartment before and after Test 1. Surficial heaving and depression could be seen in the area near the pipeline elbow and the abrupt displacement plane between the movable and fixed boxes after the test. In all cases, planes of soil slip and cracking reached the ground surface, but did not intersect the walls of the test compartment to any appreciable degree. 110 mm of surface depression and 95 mm of surface heave were measured after the test.

Fig. 6 shows an overhead view of the test compartment after soil excavation to the pipeline following Test 1. Leakage occurred at the connecting part between the elbow and the shorter straight pipe when the ground displacement was 0.78 m, and full circumferential rupture of the pipe occurred when the displacement was 0.94 m. **Fig. 7** (a) is a macrographic photograph of the fracture. Necking was observed in the pipe metal outside the heat-affected zone, but close to the crack. **Fig. 7** (b) is a SEM (Scanning Electron Microscope) photograph of the fractured surface. Dimples are clearly observed in the surface, which indicates a ductile fracture. The transverse cross-section of the elbow was oval in shape, which is remarkably consistent with the shape, which was observed in the bending experiments for elbows described in the previous work by Yoshizaki et al.^{12), 13), 14)}

Table 3 summarizes test results including ground displacement at both leakage and full pipe rupture, and maximum load at each end of the experimental pipeline. The inequality sign with the maximum reaction force at the end of the long leg for Test 1 indicates the load cell capacity of 135.3 kN. Leakage occurred during Test 2, but a full circumferential rupture of the pipe did not occur. The change in bend angle of the elbow measured after the test was -40 degrees. Test 1, in which the soil had a higher friction angle than that of Test 2, also had higher values for reaction forces at both



(a) Before experiment



(b) After experiment

Fig. 5 Overhead view of test compartment before and after the experiment (Test 1)

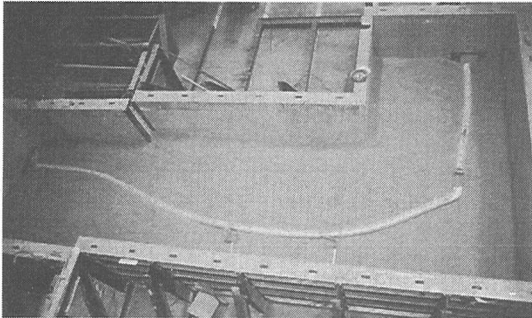


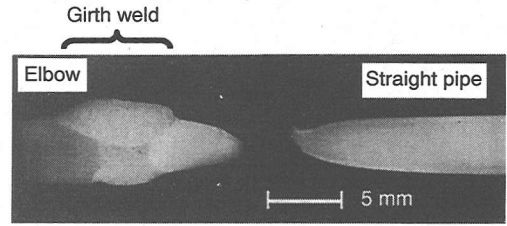
Fig. 6 Overhead view of deformed pipeline (Test 1)

ends of the pipe, and smaller ground displacement when leakage or rupture occurred.

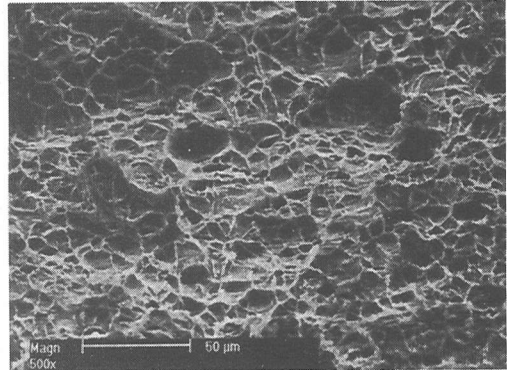
3. FINITE ELEMENT ANALYSES FOR THE LARGE-SCALE EXPERIMENTS

(1) Analytical model

Finite element analyses (hereafter, “FEA”) were conducted to calibrate and validate the analytical model. The FEA results also help to clarify key



(a) Macroscopic photograph



(b) SEM (Scanning Electron Microscope) photograph

Fig. 7 Macroscopic photograph and SEM photograph of the fractured surface

Table 3 Experimental results

	Test 1	Test 2
Ground displacement at leakage, $\delta_{g, \text{leakage}}$ (m)	0.78	0.85
Ground displacement at rupture, $\delta_{g, \text{rupture}}$ (m)	0.94	(No rupture)
Maximum reaction force at the edge of the short leg, F_{short} (kN)	144.3	132.6
Maximum reaction force at the edge of the long leg, F_{long} (kN)	> 135.3	128.0

aspects of the pipeline and elbow response to abrupt lateral displacement.

The pipeline was modeled with isotropic shell elements with reduced integration points. Average values of the actual thickness measured with an ultrasonic thickness meter were used for bend and straight pipes in the model. True stress – true strain relationships from tension test data were approximated by multi-linear trends for elbow and straight pipe, as plotted in **Fig. 8**. From the results of the previous work^{13), 14)}, seventy-two elements were employed around the pipe circumference, and the aspect ratio for the elbow and the straight pipes near the elbow was 1:1 in the axial direction. ABAQUS Version 5.8 was used as a solver for the analyses with geometric nonlinearity and large strain formulation. The von Mises criterion and

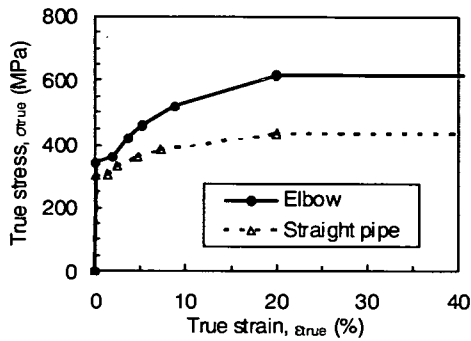


Fig. 8 Stress-strain curves for pipes used in FE modeling

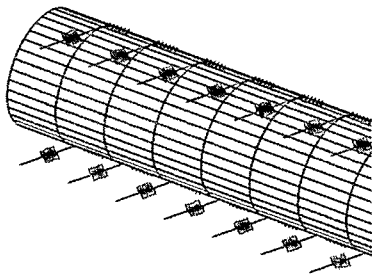


Fig. 9 Modelling of soil-pipe interaction

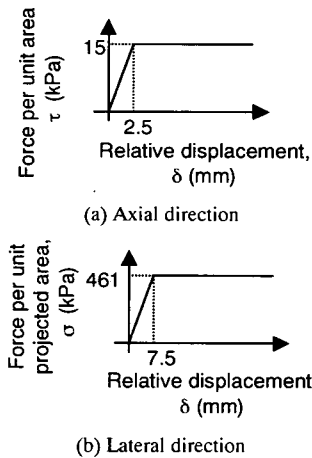
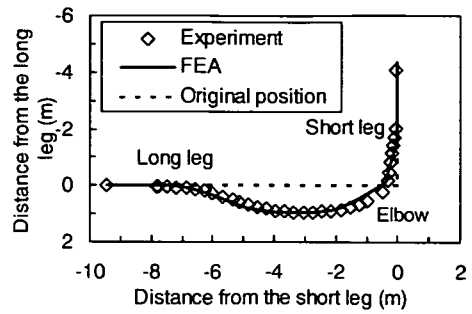


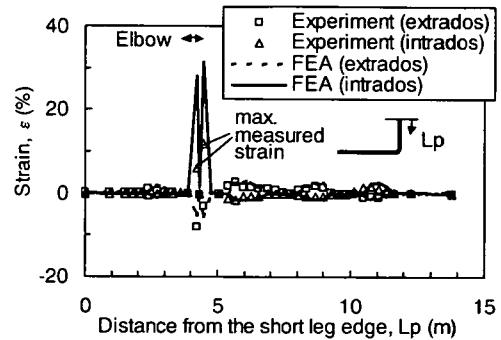
Fig. 10 Soil-pipe interaction for Test 1

associated flow rule were applied to the model. Since the straining is in the same direction in strain space throughout the analyses, isotropic hardening was used in the model. An internal pipe pressure of 0.1 MPa was also applied in the model.

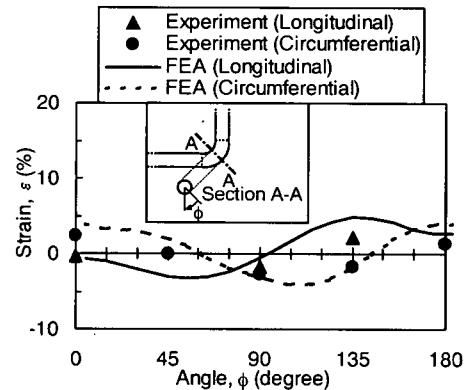
Soil-pipe interaction was modeled with spring elements, which were allocated at the top and bottom of the pipeline as shown in Fig. 9. The force-displacement relationships were modeled in accordance with JGA guideline¹⁹⁾ and the data



(a) Deformation of the pipeline after the test ($\delta_g = 0.94$ m)



(b) Distribution of axial strain in the longitudinal direction ($\delta_g = 0.78$ m)



(c) Strain distribution at the cross section of the elbow ($\delta_g = 0.78$ m)

Fig. 11 Comparison Between Analytical and Experimental Results

presented by Trautmann and O'Rourke²⁰⁾. Although the strain rate of the soil during the tests with 16 mm/s of the ground velocity is difficult to obtain, the internal friction angle obtained from the triaxial compression tests with 5%/min of strain rate was used to calculate the soil-pipe interaction. Fig. 10 (a) shows the force per unit area vs. relative displacement plot used to model soil-pipe

interaction in the axial direction. Fig. 10 (b) shows the force per unit projected area vs. relative displacement plot in the lateral direction.

(2) Analytical results for Test 1

Fig. 11 (a) compares the deformed pipeline shape of the analytical model with measured deformation of the experimental pipeline for Test 1 when the ground displacement was 0.94 m. There is excellent agreement between the two, as well as close agreement between the analytical deformation and the overhead view of the deformed pipeline in Fig. 6.

Fig. 11 (b) shows the measured and predicted longitudinal strains under maximum ground deformation on both the extrados and intrados surfaces along the pipeline when the ground displacement was 0.78 m. In this figure, the data point with a special label that indicates the maximum strain measured when electrical contact with the gage was lost during the experiment. The disconnection occurred before maximum deformation of the elbow so that the actual strain was larger than the value plotted. Fig. 11 (c) shows the measured and analytical strains around the pipe circumference in which the angular distance is measured from extrados to intrados of pipe, corresponding to 0 and 180 degrees, respectively. Overall, there is good agreement for both the magnitude and distribution of measured and analytical strains and deformation, and the analytical model was able to simulate the observed performance in a reliable way.

(3) Effect of water content

The soil deformation patterns adjacent to the pipeline were different for the dry and partially saturated sands. During PGD, the dry sand in Test 1 tended to flow around the experimental pipeline, filling the spaces behind it as relative horizontal movement of the pipe increased. In contrast, the partially saturated sand in Test 2 possessed apparent cohesion because of surface tension generated by interstitial moisture among the sand particles. As a result, relative movement of the pipe generated rupture surfaces rather than flow in the adjacent soil, which was evident in more abrupt and pronounced surface deformation after Test 2. The generation of discrete rupture surfaces in partially saturated sand would be expected to result in lateral pipe forces larger than those related to the shear flow conditions of Test 1, provided that PGD occurred under similar conditions of soil dry density and pipeline depth. To consider the difference in failure mechanism for partially saturated sand, a correction

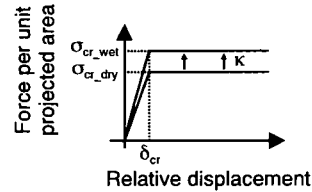


Fig. 12 Definition of correction factor of K for soil-pipe interaction in the lateral direction

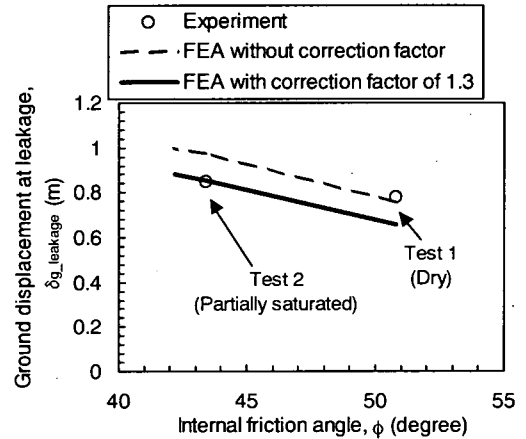


Fig. 13 Comparison between analytical results with correction factors for partially saturated sand and experimental results when the change in bend angle of the elbow is -40 degrees

factor K was adopted in the following formula:

$$\sigma_{cr_wet} = K \cdot \sigma_{cr_dry}$$

where σ_{cr_wet} and σ_{cr_dry} are the critical force per unit projected area in the lateral direction for partially saturated and dry sand, respectively, as shown in Fig. 12. Fig. 13 shows the analytical results using a correction factor of 1.3 with the results of the large scale experiments. The "corrected" analytical results show better agreement with those of the large-scale experiments than those without the correction factor.

Fig. 13 illustrates an important finding of this work in that partially saturated soils develop discrete and well-pronounced rupture patterns for the conditions represented by the experiments. This rupture pattern appears to be accompanied by increased reaction forces on buried pipelines during PGD relative to those that are generated by dry sand with similar dry density and friction angle. Comparison of the analytical and experimental results allows for the estimation of a correction factor. This factor may be used to adjust the lateral force vs displacement relationships developed from tests using dry sand to predict similar relationships for partially saturated conditions that are more representative of field performance.

4. RECOMMENDATIONS FOR ENHANCEMENT OF EARTHQUAKE RESISTANCE OF BURIED PIPELINES WITH ELBOWS

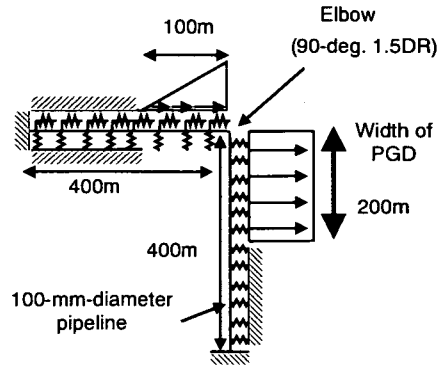
Using the calibrated analytical model, recommendations are proposed for enhancing the resistance of buried pipelines with elbows against PGD during earthquakes. Since concentrated strains can easily accumulate at elbows in response to PGD, the earthquake resistance against PGD can be improved effectively if the elbows are reinforced. As observed in both past work^{(12), (13), (14)} and the large-scale experiments described in the previous sections, leakage occurred near the welds connecting the straight pipes to the elbow. Therefore, the earthquake resistance against PGD can be improved effectively if this portion of the pipeline is reinforced.

First of all, the effect of reinforcement by using straight pipes with increased wall thickness near the elbow was investigated. **Fig. 14** (a) shows the assumed model of a 100-mm-diameter pipeline with an elbow subjected to PGD. The configuration of the straight pipes with increased thickness is shown in **Fig. 14** (b). **Table 4** lists the analytical cases used to investigate the effect of larger wall thickness for straight pipes. The standard thickness of the straight pipe for SGP steel (JIS-G3452) is 4.5 mm, which corresponds to Case 1 in the table. Case 2 is the analytical case with an increased thickness of 6.0mm using STPT 370 Schedule 40 steel (JIS-G3456) for straight pipes that extend a short distance of 0.1 m from the elbow. The effect of length was also investigated by analyzing lengths of larger-thickness straight pipes of 0.5 m and 400 m, corresponding to Cases 3 and 4, respectively. Relationships for dry sand with internal friction angle of 40 degrees, as shown in **Fig. 15** (a) and (b), were used for soil-pipe interaction in the axial and the lateral directions, respectively, to assume a field condition.

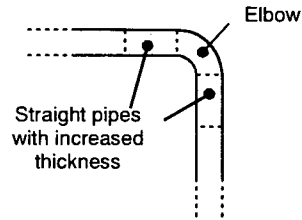
Fig. 16 (a) shows the analytical results for the four cases listed in **Table 4**. The strain is defined as equivalent plastic strain, which is given by the following formulas:

$$\varepsilon_{eq}^p = \int d\varepsilon_{eq}^p$$

$$d\varepsilon_{eq}^p = \sqrt{\frac{1}{3} \left\{ 4 \left(d\varepsilon_c^{p2} + d\varepsilon_l^{p2} + d\varepsilon_{ct}^{p2} \right) + d\gamma_{ct}^{p2} \right\}}$$



(a) Assumed model



(b) Configuration of straight pipes with increased thickness

Fig. 14 Assumed model on the effect of elbow and straight pipes with increased thickness

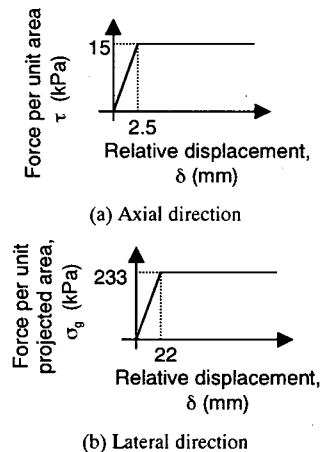


Fig. 15 Model of soil-pipe interaction for 100-mm-diameter pipe with cover depth of 0.9 m and internal friction angle of 40 degrees

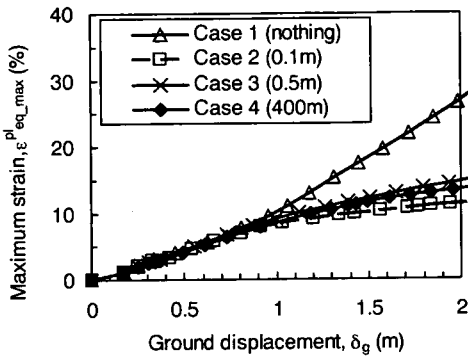
where ε_c^p and ε_l^p are plastic strain in the circumferential, longitudinal directions, respectively, and γ_{ct}^p is the plastic shear strain. **Fig. 16** (b) summarizes the maximum strain when the ground displacement is 1 m and 2 m for all cases. Here, the maximum strain of 30% was verified with the large-scale experiments described in the previous sections. The strain is reduced significantly by the use of straight pipes with increased thickness, and

Table 4 Analytical cases on the effect of straight pipes with increased thickness

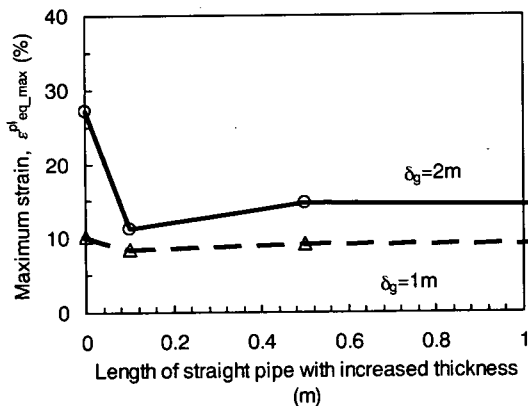
	Thickness	
	Elbow	Straight pipes
Case 1	5.4 mm	4.5 mm for all of the straight pipes
Case 2	5.4 mm	6.0 mm for 0.1m from the elbow 4.5 mm for others
Case 3	5.4 mm	6.0 mm for 0.5m from the elbow 4.5 mm for others
Case 4	5.4 mm	6.0 mm for all of the straight pipes

Table 5 Analytical cases on the effect of elbows with increased thickness

	Thickness	
	Elbow	Straight pipes
Case 1	5.4 mm	4.5 mm for all of the straight pipes
Case 2	5.4 mm	6.0 mm for 0.1m from the elbow 4.5 mm for others
Case 5	6.0 mm	4.5mm for all of the straight pipes
Case 6	6.0 mm	6.0 mm for 0.1m from the elbow 4.5 mm for others



(a) Maximum strain vs. ground displacement

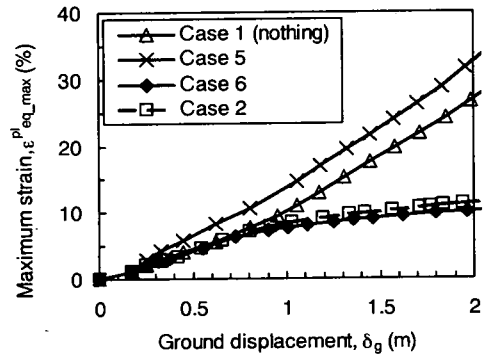


(b) Maximum strain at the ground displacement of 1m and 2m

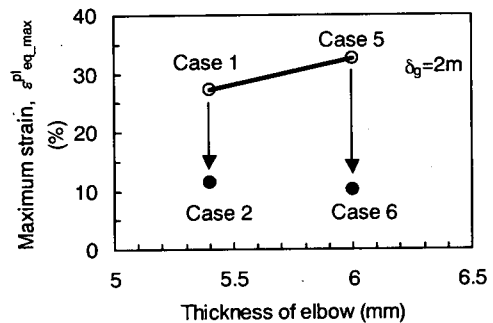
Fig. 16 Analytical results on the effect of straight pipes with increased thickness

the effect is notable even when the length of increased thickness pipe is only 0.1 m from the elbow.

Table 5 summarizes the analytical cases to investigate the effects of increased elbow thickness. **Fig. 17** plots the maximum pipe strain derived from these analyses as a function of both ground displacement and pipe wall thickness. Increasing the elbow wall thickness without similar increases in



(a) Maximum strain vs. ground displacement



(b) Maximum strain at the ground displacement of 2 m

Fig. 17 Analytical results on the effect of elbow and straight pipes with increased thickness

the straight pipes (Case 5), which connect to the elbow, actually reduces the resistance of the pipeline against ground displacement. This behavior can be explained by reference to the deformation of elbows in the opening mode previously reported for bending experiments^{(12), (13), (14)}. Because of the change in central cross-sectional shape during opening mode flexure, the stiffness of the elbow becomes larger than that of the straight pipes connected to it. Bending strains are then concentrated at the location where the straight pipes join the elbow. If the thickness of the elbow is increased, its bending

stiffness also increases as it deforms into an oval cross-section. Therefore, large bending strains are induced at the location where the straight pipe and elbow are joined at an earlier stage in the deformation process.

If straight pipes with the same thickness as the elbow are used over a distance of 0.1 m from the elbow (Case 6), the maximum strain for a ground displacement of 2 m is smaller than the strains of Cases 2 and 5, as shown by the arrows in Fig. 17 (b). These results indicate that thicker wall pipe is effective for enhancing earthquake-resistance when elbows and straight pipes of increased thickness are combined for short distances from the elbow. Combining elbows and end sections of straight pipe, both of which have increased wall thickness, removes structural unevenness at the location where strain concentration occurs.

5. CONCLUSIONS

This paper describes large-scale experiments to investigate the effects of PGD on buried steel pipelines with elbows during earthquakes, and to validate and calibrate analytical models. A 100-mm-diameter pipeline with an elbow of 90 degrees of initial bend angle was buried with 0.9 m of cover depth and 0.1 MPa of internal pressure, and subjected to 1 m of ground displacement simulating PGD. The following conclusions are drawn in this study.

- (1) For dry sand with internal friction angle of 51 degrees, leakage occurred at the connecting part between the elbow and the shorter straight pipe when the ground displacement was 0.78 m. The transverse cross-section of the elbow deformed into an oval remarkably consistent with the shape, previously observed in bending experiments for elbows^{(12), (13), (14)}.
- (2) Finite Element analyses (FEA) were performed to simulate the deformation behavior of buried pipelines with elbows subjected to PGD using shell elements for pipes and spring elements for soil-pipe interaction. There was good agreement for both the magnitude and distribution of measured and analytical strains and deformation, and the analytical model was able to simulate full-scale performance in a reliable way.
- (3) Partially saturated soils developed discreet and well-pronounced rupture patterns that appeared to be accompanied by lateral forces on buried pipelines during PGD that were larger than those generated in dry sand under similar conditions. Comparison of the analytical and experimental results of this work allows for the

estimation of a correction factor. The factor can be used to adjust the lateral force vs displacement relationships from tests using dry sand to partially saturated conditions that are more representative of field performance.

- (4) Using the experimentally calibrated analytical model, a parametric study was conducted to evaluate ways of enhancing the earthquake-resistance of buried pipelines with elbows subjected to PGD. An effective means of PGD reinforcement is to use straight pipe with wall thickness the same as or more than that of the elbow for a distance of 0.1 m from the elbow. This type of fabrication removes structural unevenness at the locations where strain tend to concentrate.

ACKNOWLEDGMENT: The authors wish to thank Messrs. Noritake Oguchi, Tomoki Masuda, Takahito Watanabe, Hirokazu Ando, Hiroshi Sugawara, Naoto Hagiwara, Hiroshi Yatabe, Naoyuki Hosokawa and Naoki Fukuda of Tokyo Gas Co., Ltd. for their assistance. This research was conducted using the resources of the Winter Structural Laboratory at Cornell University. Thanks are extended to Messrs. Tim Bond and James Mason of Cornell for their invaluable assistance in conducting the experiments. The research was sponsored in part by the Multidisciplinary Center for Earthquake Engineering Research (MCEER), Buffalo, NY and by the National Science Foundation through the US-Japan Cooperative Research Program on Mitigation of Urban Earthquake Disasters. Resources were also provided by the Cornell Theory Center, which receives funding from Cornell University, New York State, the National Center for Research Resources at the National Institutes of Health, the National Science Foundation, the Defense Department Modernization Program, the United States Department of Agriculture, and corporate partners.

REFERENCES

- 1) Youd, T. L. and Hoose, S. N.: Historic Ground Failures in Northern California Triggered by Earthquakes, Geological Survey Professional Paper 993, U. S. Government Printing Office, Washington, D. C., 177 p., 1978.
- 2) O'Rourke, T. D. and Lane, P. A.: Liquefaction Hazards and Their Effects on Buried Pipelines, *Technical Report*, NCEER-89-0007, NCEER, Buffalo, NY, 1989.
- 3) Hamada, M.: Large Ground Deformations and Their Effects on Lifeline: 1964 Niigata Earthquake, *Proceedings*, Case Studies of Liquefaction and Lifeline Performance During Past Earthquakes, Volume 1, Japanese Case Studies,

- MCEER-92-0001, NCEER, Buffalo, NY, 1992.
- 4) O'Rourke, T. D., Roth, B. L. and Hamada, M.: Large Ground Deformations and Their Effects on Lifeline Facilities: 1971 San Fernando Earthquake, *Proceedings, Case Studies of Liquefaction and Lifeline Performance During Past Earthquakes, Volume 2, United States Case Studies*, MCEER-92-0002, NCEER, Buffalo, NY, 1992.
 - 5) Dobry, R., Baziar, M. H., O'Rourke, T. D., Roth, B. L. and Youd, T. L.: Liquefaction and Ground Failure in the Imperial Valley, Southern California During the 1979, 1981 and 1987 Earthquakes, *Proceedings, Case Studies of Liquefaction and Lifeline Performance During Past Earthquakes, Volume 2, United States Case Studies*, MCEER-92-0002, NCEER, Buffalo, NY, 1992.
 - 6) O'Rourke, T. D. and Palmer, M. C.: Earthquake Performance of Gas Transmission Pipelines, *Earthquake Spectra*, Vol. 20, No. 3, pp. 493-527, 1996.
 - 7) Hamada, M.: Large Ground Deformations and Their Effects on Lifeline: 1989 Nihonkai-Chubu Earthquake, *Proceedings, Case Studies of Liquefaction and Lifeline Performance During Past Earthquakes, Volume 1, Japanese Case Studies*, MCEER-92-0001, NCEER, Buffalo, NY, 1992.
 - 8) O'Rourke, T. D. and Pease, J. W.: Large Ground Deformations and Their Effects on Lifeline Facilities: 1989 Loma Prieta Earthquake, *Proceedings, Case Studies of Liquefaction and Lifeline Performance During Past Earthquakes, Volume 2, United States Case Studies*, MCEER-92-0002, NCEER, Buffalo, NY, 1992.
 - 9) O'Rourke, T. D., Toprak, S. and Sano, Y.: Los Angeles Water Pipeline System Response to the 1994 Northridge Earthquake, *Proceedings, 6th Japan-U.S. Workshop on Earthquake Resistant Design of Lifeline Facilities and Countermeasures Against Soil Liquefaction*, MCEER-96-0012, NCEER, Buffalo, NY, 1996.
 - 10) Oka, S.: Damage of Gas Facilities by Great Hanshin Earthquake and Restoration Process, *Proceedings, 6th Japan-U.S. Workshop on Earthquake Resistant Design of Lifeline Facilities and Countermeasures Against Soil Liquefaction*, NCEER-96-0012, MCEER, Buffalo, NY, pp.111-124, 1996.
 - 11) Japan Society of Civil Engineers: The 1999 Ji-Ji Earthquake, Taiwan, Investigation into the damage to civil engineering structures, *Investigation Report*, pp. 7.13-7.21, 1999.
 - 12) Yoshizaki, K., Hamada, M. and O'Rourke, T. D.: Large Deformation Behavior of Pipelines with Elbows, *Proceedings, 5th U.S. Conference on Lifeline Earthquake Engineering*, ASCE, Reston, VA, 1999.
 - 13) Yoshizaki, K., Hosokawa, N., Ando, H., Oguchi, N., Sogabe, K. and Hamada, M.: Deformation behavior of buried pipelines with elbows subjected to large ground deformation, *Journal of Structural Mechanics and Earthquake Engineering* (in Japanese), JSCE, No. 626/I-48, pp. 173-184. 1999.
 - 14) Yoshizaki, K., O'Rourke, T. D. and Hamada, M.: Large Deformation Behavior of Buried Pipelines with Low-angle Elbows Subjected to Permanent Ground Deformation, *Journal of Structural Mechanics and Earthquake Engineering*, Vol. 18, No. 1, No. 675/I-55, pp. 41-52, 2001.
 - 15) Yoshizaki, K. and Oguchi, N.: Estimation of the deformation behavior of elbows for an earthquake-resistant design, *Proceedings, 11th World Conference on Earthquake Engineering*, Acapulco, Mexico, Paper No. 1783, Elsevier Science, 1996.
 - 16) Japan Gas Association: *Recommended Practice for Earthquake Resistant Design of High Pressure Gas Pipelines against Ground Liquefaction (draft)*, Japan Gas Association (in Japanese), Tokyo, Japan, 2001.
 - 17) Suzuki, N. and Ohba, S.: Low Cycle Fatigue Strength of Welded Elbows Subjected to In-plane Bending, *Journal of Structural Engineering*, Vol. 36A, pp. 1355-1364, 1990 (in Japanese).
 - 18) Japan Gas Association: *Recommended Practice for Earthquake Resistant Design of Gas Pipeline*, Japan Gas Association (in Japanese), Tokyo, Japan, 1982.
 - 19) Japan Gas Association: *Recommended Practice for Earthquake Resistant Design of High Pressure Gas Pipelines*, Japan Gas Association (in Japanese), Tokyo, Japan, 2000.
 - 20) Trautmann, C. H. and O'Rourke, T. D.: Lateral force-displacement response of buried pipe, *Journal of Geotechnical Engineering*, ASCE, Reston, VA, Vol. 111, No.9, pp. 1077-1092, 1985.

(Received February 14, 2002)

永久地盤変位を受けた埋設曲管配管系についての大規模実験

吉崎浩司・Thomas D. O'ROURKE・濱田政則

地震時に大規模な永久地盤変位を受けた場合の曲管を有する埋設パイプラインの大変形挙動について、実規模での実験により評価を行った。乾燥砂および湿潤砂にて作成した地盤中に曲管を有する溶接鋼管を埋設し永久地盤変位を与えたところ、曲管部は外曲げ方向に大きく変形し、その変形挙動は曲管単体での曲げ変形挙動とほぼ同等であった。また管をシェル要素、地盤をばね要素にてモデル化した数値解析を実施したところ、パイプラインの変形挙動を精度良く再現することができた。更に構築した数値解析モデルを用いた解析的検討を実施し、耐震性を向上する手法について提案を行った。